

High-Dimensional Architectures from the Self-Assembly of Lanthanide Ions with Benzenedicarboxylates and 1,10-Phenanthroline

Yonghong Wan,[†] Liping Zhang,^{†,‡} Linpei Jin,^{*,†} Song Gao,[§] and Shaozhe Lu^{||}

Departments of Chemistry, Beijing Normal University, Beijing 100875, and Anyang Teacher College, Henan 455000, State Key Laboratory of Rare Earth Materials Chemistry and Applications, Peking University, Beijing 100871, and Laboratory of Excited States Processes, Chinese Academy of Sciences, Changchun 130021, People's Republic of China

Received March 10, 2003

Six new coordination polymers, [Eu(1,2-BDC)(1,2-HBDC)(phen)(H₂O)]_n (**1**), [Eu₂(1,3-BDC)₃(phen)₂(H₂O)₂]_n·4nH₂O (**2**), [Eu(1,4-BDC)_{3/2}(phen)(H₂O)]_n (**3**), [Yb₂(1,2-BDC)₃(phen)(H₂O)₂]_n·3.5nH₂O (**4**), [Yb₂(1,3-BDC)₃(phen)_{1/2}]_n (**5**), and [Yb₂(1,4-BDC)₃(phen)₂(H₂O)]_n (**6**), were synthesized by hydrothermal reactions of lanthanide chlorides with three isomers of benzenedicarboxylic acid (H₂BDC) and 1,10-phenanthroline (phen), and characterized by single-crystal X-ray diffraction. **1** has a 2-D herringbone architecture with a Z-shaped cavity. **2** and **5** have different 3-D networks, but both are formed by 1,3-BDC anions bridging metal centers (Eu or Yb) via carboxylate groups. **3** and **6** possess similar layer structures which are further constructed to form 3-D networks by hydrogen bonds and/or π - π aromatic interactions. **4** comprises 1-D chains that are further interlinked via hydrogen bonds, resulting in a 3-D network. In the three europium complexes, all the europium ions are eight-coordinated, while the coordination numbers of the ytterbium ions in other three-coordination polymers range from six to eight. Crystal data: for **1**, monoclinic, space group *P*2₁/*c*, with *a* = 12.565(6) Å, *b* = 16.005(8) Å, *c* = 12.891(6) Å, β = 102.173(8)°, and *Z* = 4; for **2**, monoclinic, space group *P*2₁/*c*, with *a* = 20.979(4) Å, *b* = 11.5989(19) Å, *c* = 20.810(3) Å, β = 110.391(3)°, and *Z* = 4; for **3**, triclinic, space group *P* $\bar{1}$, with *a* = 10.331(5) Å, *b* = 10.887(5) Å, *c* = 11.404(5) Å, α = 107.660(7)°, β = 91.787(7)°, γ = 112.946(6)°, and *Z* = 2; for **4**, triclinic, space group *P* $\bar{1}$, with *a* = 11.517(5) Å, *b* = 13.339(5) Å, *c* = 13.595(6) Å, α = 87.888(7)°, β = 67.759(6)°, γ = 68.070(6)°, and *Z* = 2; for **5**, orthorhombic, space group *C*222₁, with *a* = 8.174(2) Å, *b* = 24.497(7) Å, *c* = 29.161(8) Å, and *Z* = 8; for **6**, triclinic, space group *P* $\bar{1}$, with *a* = 10.349(3) Å, *b* = 11.052(3) Å, *c* = 19.431(6) Å, α = 105.464(4)°, β = 91.300(5)°, γ = 93.655(5)°, and *Z* = 2. The magnetic properties of **1** and **4** were investigated. The photophysical properties of **1** were also studied.

Introduction

The construction of coordination polymers has been a field of rapid growth in supramolecular and materials chemistry due to the formation of fascinating structures and potential applications as new materials.¹ Benzenedicarboxylate (BDC)

anions as linkers have been widely used in construction of coordination polymers containing transition metals because of their versatile coordination modes. A series of transition-metal complexes with 1,4-BDC,² 1,3-BDC,³ and 1,2-BDC⁴ have been reported. In contrast to transition-metal benzenedicarboxylate complexes, lanthanide complexes with BDC

* Author to whom correspondence should be addressed. Phone: +86-010-62205522. Fax: +86-010-62200567. E-mail: lpjin@bnu.edu.cn.

[†] Beijing Normal University.

[‡] Anyang Teacher College.

[§] Peking University.

^{||} Chinese Academy of Sciences.

(1) (a) Moulton, B.; Zaworotko, M. J. *Chem. Rev.* **2001**, *101*, 1629–1658. (b) Eddaoudi, M.; Moler, D. B.; Li, H.; Chen, B.; Reineke, T. M.; O'Keeffe, M.; Yaghi, O. M. *Acc. Chem. Res.* **2001**, *34*, 319–330. (c) Yaghi, O. M.; Li, H.; Davis, C.; Richardson, D.; Groy, T. L. *Acc. Chem. Res.* **1998**, *31*, 474–484.

(2) (a) Li, H.; Eddaoudi, M.; O'Keeffe, M.; Yaghi, O. M. *Nature* **1999**, *402*, 276–279. (b) Eddaoudi, M.; Kim, J.; Rosi, N.; Vodak, D.; Wachter, J.; O'Keeffe, M.; Yaghi, O. M. *Science* **2002**, *295*, 469–472. (c) Li, H.; Eddaoudi, M.; Groy, T. L.; Yaghi, O. M. *J. Am. Chem. Soc.* **1998**, *120*, 8571–8572. (d) Li, H.; Davis, C. E.; Groy, T. L.; Kelley, D. G.; Yaghi, O. M. *J. Am. Chem. Soc.* **1998**, *120*, 2186–2187. (e) Edgar, M.; Mitchell, R.; Slawin, A. M. Z.; Lightfoot, P.; Wright, P. A. *Chem.—Eur. J.* **2001**, *7*, 5168–5175. (f) Barthelet, K.; Marrot, J.; Riou, D.; Férey, G. *Angew. Chem., Int. Ed.* **2002**, *41*, 281–284.

are much less studied.⁵ Owing to large radii, high coordination numbers, special fluorescence, and the magnetic properties of lanthanides, lanthanide coordination polymers have attracted considerable interest. In this work, we select benzenedicarboxylic acids with different positions of carboxyl groups on the benzene ring and 1,10-phenanthroline as mixed ligands, on the basis of the following considerations: (i) benzenedicarboxylate anions have two carboxylate groups, and they may act as linkers to connect metal ions into higher dimensional structures via varied coordination fashions; (ii) benzenedicarboxylate anions may take different effects in the construction of coordination polymers due to the different positions of the carboxylate groups on the benzene ring; (iii) phenanthroline (phen) is a good ligand for lanthanide ions and can construct supramolecular structure via C–H···O hydrogen bonds and π – π aromatic interactions.⁶ Therefore, we selected the two compounds as mixed ligands and hope to construct novel lanthanide coordination polymers with fascinating structures and/or characteristic properties.

Hydrothermal synthesis has been employed in this field to obtain single crystals because of the obvious advantages over other methods.⁷ Even insoluble reagents which are unsuitable to synthesize complexes by conventional means can be used in this method, and in the reaction process metastable compounds may be produced and thus are liable to crystal growth. Herein we report the syntheses and structural characterizations of six lanthanide benzenedicarboxylate complexes with 1,10-phenanthroline, [Eu(1,2-BDC)(1,2-HBDC)(phen)(H₂O)]_n (**1**), [Eu₂(1,3-BDC)₃(phen)₂(H₂O)₂]_n·4nH₂O (**2**), [Eu(1,4-BDC)_{3/2}(phen)(H₂O)]_n (**3**), [Yb₂(1,2-BDC)₃(phen)(H₂O)₂]_n·3.5nH₂O (**4**), [Yb₂(1,3-BDC)_{3/2}(phen)_{1/2}]_n (**5**), and [Yb₂(1,4-BDC)₃(phen)₂(H₂O)]_n (**6**).

Experimental Section

Materials and Apparatus. EuCl₃·6H₂O and YbCl₃·6H₂O were prepared by dissolving lanthanide oxide in dilute hydrochloric acid and dried. Other chemicals for the synthesis were commercially available and used without further purification. Elemental analyses (C, H, N) were performed on a Vario EL elemental analyzer, and infrared spectra were recorded on a Nicolet Avatar 360 FT-IR spectrometer. The temperature dependence of magnetic susceptibility and field dependence of magnetization for crystalline samples were recorded on an Oxford MagLab 2000 magnetometer in the temperature range of 2–300 K. The luminescence spectra were recorded at 77 K using a YAG:Nd laser with an excitation wavelength of 355 nm and a SPEX 1403 double grating monochromator.

Synthesis of Complexes. [Eu(1,2-BDC)(1,2-HBDC)(phen)(H₂O)]_n (**1**). A 0.110 g sample of EuCl₃·6H₂O (0.3 mmol), 0.075 g of 1,2-H₂BDC (0.45 mmol), 0.059 g of phen (0.3 mmol), 0.8 mL of a 0.51 M NaOH aqueous solution (0.4 mmol), and 10 mL of deionized water were sealed in a Teflon-lined stainless steel vessel (25 mL), heated at 150 °C for 5 d under autogenous pressure, and then cooled slowly to room temperature. Colorless and sheetlike crystals were collected by filtration and washed with deionized water and ethanol. Yield: 89 mg (58%). Anal. Found: C, 49.46; H, 2.57; N, 3.94. Calcd: C, 49.49; H, 2.82; N, 4.12. IR (KBr pellet, cm⁻¹): 3530m(br), 1725m, 1623s, 1573m, 1540s, 1429s, 1391s, 1337m, 841m, 726m.

[Eu₂(1,3-BDC)₃(phen)₂(H₂O)₂]_n·4nH₂O (**2**). A 0.112 g sample of EuCl₃·6H₂O (0.3 mmol), 0.075 g of 1,3-H₂BDC (0.45 mmol), 0.059 g of phen (0.3 mmol), 0.8 mL of a 0.51 M NaOH aqueous solution (0.4 mmol), and 10 mL of deionized water were sealed in a Teflon-lined stainless steel vessel (25 mL), heated at 150 °C for 5 d under autogenous pressure, and then cooled slowly to room temperature. Colorless and needlelike crystals were obtained and washed with deionized water and ethanol. Yield: 69 mg (36%). Anal. Found: C, 45.59; H, 2.57; N, 4.31. Calcd: C, 45.58; H, 3.19; N, 4.43. IR (KBr pellet, cm⁻¹): 3416m(br), 1624s, 1546m, 1444m, 1388s, 1143w, 864w, 849m, 752m, 700m, 655w.

[Eu(1,4-BDC)_{3/2}(phen)(H₂O)]_n (**3**). A 0.111 g sample of EuCl₃·6H₂O (0.3 mmol), 0.050 g of 1,4-H₂BDC (0.3 mmol), 0.059 g of phen (0.3 mmol), 0.7 mL of a 0.65 M NaOH aqueous solution (0.5 mmol), and 10 mL of deionized water were sealed in a Teflon-lined stainless steel vessel (25 mL), heated at 190 °C for 1 d and 180 °C for 1 d under autogenous pressure, and then cooled slowly to room temperature. Colorless and sticklike crystals were obtained and washed with ethanol. Yield: 35 mg (29%). Anal. Found: C, 48.07; H, 2.35; N, 4.90. Calcd: C, 48.33; H, 2.70; N, 4.70. IR (KBr pellet, cm⁻¹): 3443m(br), 1639m, 1589m, 1550m, 1501m, 1393s, 1141w, 1101w, 844m, 750m, 730m, 636w.

[Yb₂(1,2-BDC)₃(phen)(H₂O)₂]_n·3.5nH₂O (**4**). A 0.114 g sample of YbCl₃·6H₂O (0.3 mmol), 0.075 g of 1,2-H₂BDC (0.45 mmol), 0.059 g of phen (0.3 mmol), 1.2 mL of a 0.65 M NaOH aqueous solution (0.8 mmol), and 10 mL of deionized water were sealed in a Teflon-lined stainless steel vessel (25 mL), heated at 150 °C for 3 d under autogenous pressure, and then cooled slowly to room temperature. Colorless and sheetlike crystals were collected and washed with deionized water and ethanol. Yield: 151 mg (90%). Anal. Found: C, 39.62; H, 2.38; N, 2.59. Calcd: C, 39.64; H, 2.59; N, 2.57. IR (KBr pellet, cm⁻¹): 3440m(br), 1615s, 1566s, 1536s, 1479m, 1425s, 1408s, 1373m, 865w, 846w, 728m, 698w.

[Yb₂(1,3-BDC)₃(phen)_{1/2}]_n (**5**). A 0.156 g sample of YbCl₃·6H₂O (0.4 mmol), 0.066 g of 1,3-H₂BDC (0.4 mmol), 0.080 g of phen (0.4 mmol), 0.7 mL of a 0.65 M NaOH aqueous solution (0.5

- (3) (a) Eddaoudi, M.; Kim, J.; Wachter, J. B.; Chae, H. K.; O'Keeffe, M.; Yaghi, O. M. *J. Am. Chem. Soc.* **2001**, *123*, 4368–4369. (b) Bourne, S. A.; Lu, J.; Mondal, A.; Moulton, B.; Zaworotko, M. J. *Angew. Chem., Int. Ed.* **2001**, *40*, 2111–2113. (c) Yang, S. Y.; Long, L. S.; Huang, R. B.; Zheng, L. S. *Chem. Commun.* **2002**, 472–473. (d) Otto, T. J.; Wheeler, K. A. *Acta Crystallogr.* **2001**, *C57*, 704–705. (e) Nie, J.; Liu, L.; Luo, Y.; Xu, D. *J. Coord. Chem.* **2001**, *53*, 365–371. (f) Tan, X.-S.; Sun, J.; Xiang, D.-F.; Tang, W.-X. *Inorg. Chim. Acta* **1997**, *255*, 157–161.
- (4) (a) Suresh, E.; Boopalan, K.; Jasra, R. V.; Bhadbhade, M. M. *Inorg. Chem.* **2001**, *40*, 4078–4080. (b) Bakalbassis, E. G.; Paschalidis, D. G. *Inorg. Chem.* **1998**, *37*, 4735–4737. (c) Baca, S. G.; Simonov, Y. A.; Gerbeleu, N. V.; Gdaniec, M.; Bourosh, P. N.; Timco, G. A. *Polyhedron* **2001**, *20*, 831–837.
- (5) (a) Pan, L.; Zheng, N.-W.; Wu, Y.-G.; Han, S.; Yang, R.-Y.; Huang, X.-Y.; Li, J. *Inorg. Chem.* **2001**, *40*, 828–830. (b) Reineke, T. M.; Eddaoudi, M.; Fehr, M.; Kelley, D.; Yaghi, O. M. *J. Am. Chem. Soc.* **1999**, *121*, 1651–1657. (c) Serre, C.; Millange, F.; Marrot, J.; Férey, G. *Chem. Mater.* **2002**, *14*, 2409–2415.
- (6) (a) Chu, D.-Q.; Xu, J.-Q.; Duan, L.-M.; Wang, T.-G.; Tang, A.-Q.; Ye, L. *Eur. J. Inorg. Chem.* **2001**, 1135–1137. (b) Shi, Q.; Cao, R.; Sun, D.-F.; Hong, M.-C.; Liang, Y.-C. *Polyhedron* **2001**, *20*, 3287–3293. (c) Zheng, Y.; Sun, J.; Lin, J. Z. *Anorg. Allg. Chem.* **2000**, *626*, 1501–1504. (d) Zheng, Y.; Sun, J.; Lin, J. Z. *Anorg. Allg. Chem.* **2000**, *626*, 816–818.
- (7) (a) Pan, L.; Huang, X.; Li, J.; Wu, Y.; Zheng, N. *Angew. Chem., Int. Ed.* **2000**, *39*, 527–530. (b) Liang, Y.-C.; Cao, R.; Su, W.-P.; Hong, M.-C.; Zhang, W.-J. *Angew. Chem., Int. Ed.* **2000**, *39*, 3304–3307. (c) Cao, R.; Sun, D.; Liang, Y.; Hong, M.; Tatsumi, K.; Shi, Q. *Inorg. Chem.* **2002**, *41*, 2087–2094. (d) Wan, Y.-H.; Jin, L.-P.; Wang, K.-Z.; Zhang, L.-P.; Zheng, X.-Z.; Lu, S.-Z. *New J. Chem.* **2002**, *26*, 1590–1596.

Table 1. Crystallographic Data and Structural Refinements for 1–6

| | 1 | 2 | 3 | 4 | 5 | 6 |
|--|--|--|--|--|--|--|
| empirical formula | C ₂₈ H ₁₉ N ₂ O ₉ Eu | C ₄₈ H ₄₀ N ₄ O ₁₈ Eu ₂ | C ₂₄ H ₁₆ N ₂ O ₇ Eu | C ₃₆ H ₃₁ N ₂ O _{17.5} Yb ₂ | C ₃₀ H ₁₆ NO ₁₂ Yb ₂ | C ₄₈ H ₃₀ N ₄ O ₁₃ Yb ₂ |
| fw | 679.41 | 1264.76 | 596.35 | 1117.71 | 928.52 | 1216.84 |
| <i>T</i> /K | 293(2) | 293(2) | 293(2) | 293(2) | 293(2) | 293(2) |
| θ range/deg | 2.06–25.02 | 1.98–25.03 | 1.90–25.03 | 2.07–25.03 | 1.40–23.31 | 1.93–25.35 |
| cryst syst | monoclinic | monoclinic | triclinic | triclinic | orthorhombic | triclinic |
| space group | <i>P</i> 2 ₁ / <i>c</i> | <i>P</i> 2 ₁ / <i>c</i> | <i>P</i> $\bar{1}$ | <i>P</i> $\bar{1}$ | <i>C</i> 222 ₁ | <i>P</i> $\bar{1}$ |
| <i>a</i> /Å | 12.565(6) | 20.979(4) | 10.331(5) | 11.517(5) | 8.174(2) | 10.349(3) |
| <i>b</i> /Å | 16.005(8) | 11.5989(19) | 10.887(5) | 13.339(5) | 24.497(7) | 11.052(3) |
| <i>c</i> /Å | 12.891(6) | 20.810(3) | 11.404(5) | 13.595(6) | 29.161(8) | 19.431(6) |
| α /deg | 90 | 90 | 107.660(7) | 87.888(7) | 90 | 105.464(4) |
| β /deg | 102.173(8) | 110.391(3) | 91.787(7) | 67.759(6) | 90 | 91.300(5) |
| γ /deg | 90 | 90 | 112.946(6) | 68.070(6) | 90 | 93.655(5) |
| <i>V</i> /Å ³ | 2534(2) | 4746.5(14) | 1109.1(9) | 1779.9(12) | 5839(3) | 2135.9(12) |
| <i>Z</i> | 4 | 4 | 2 | 2 | 8 | 2 |
| <i>D</i> _{calcd} /(Mg/m ^{−3}) | 1.781 | 1.771 | 1.786 | 2.085 | 2.112 | 1.892 |
| μ /mm ^{−1} | 2.536 | 2.700 | 2.877 | 5.308 | 6.435 | 5.517 |
| <i>F</i> (000) | 1344 | 2504 | 586 | 1082 | 3512 | 1180 |
| <i>R</i> _{int} | 0.0538 | 0.0473 | 0.0220 | 0.0357 | 0.0518 | 0.0385 |
| <i>R</i> indices | <i>R</i> 1 = 0.0404 | <i>R</i> 1 = 0.0298 | <i>R</i> 1 = 0.0353 | <i>R</i> 1 = 0.0462 | <i>R</i> 1 = 0.0357 | <i>R</i> 1 = 0.0386 |
| [<i>I</i> > 2 σ (<i>I</i>)] | w <i>R</i> 2 = 0.0854 | w <i>R</i> 2 = 0.0586 | w <i>R</i> 2 = 0.1296 | w <i>R</i> 2 = 0.1058 | w <i>R</i> 2 = 0.0735 | w <i>R</i> 2 = 0.0758 |
| <i>R</i> indices (all data) | <i>R</i> 1 = 0.0717 | <i>R</i> 1 = 0.0482 | <i>R</i> 1 = 0.0420 | <i>R</i> 1 = 0.0721 | <i>R</i> 1 = 0.0492 | <i>R</i> 1 = 0.0680 |
| | w <i>R</i> 2 = 0.0962 | w <i>R</i> 2 = 0.640 | w <i>R</i> 2 = 0.1345 | w <i>R</i> 2 = 0.1186 | w <i>R</i> 2 = 0.0856 | w <i>R</i> 2 = 0.0834 |

mmol), and 12 mL of deionized water were sealed in a Teflon-lined stainless steel vessel (25 mL), heated at 150 °C for 5 d, and then cooled to room temperature. Colorless and needlelike crystals were obtained and washed with ethanol. Yield: 81 mg (44%). Anal. Found: C, 38.68; H, 1.32; N, 1.30. Calcd: C, 38.79, H, 1.74, N, 1.51. IR (KBr pellet, cm^{−1}): 3430m(br), 1658m, 1598m, 1573m, 1544m, 1452m, 1405s, 1277w, 853m, 746m, 701m, 653m.

[Yb₂(1,4-BDC)₃(phen)₂(H₂O)_n (6). A 0.114 g sample of YbCl₃·6H₂O (0.3 mmol), 0.050 g of 1,4-H₂BDC (0.3 mmol), 0.059 g of phen (0.3 mmol), 0.7 mL of a 0.65 M NaOH aqueous solution (0.5 mmol), and 10 mL of deionized water were sealed in a Teflon-lined stainless steel vessel (25 mL), heated at 160 °C for 3 d, and then cooled slowly to room temperature. Colorless and rhombus crystals were obtained and washed with ethanol. Yield: 18 mg (15%). Anal. Found: C, 46.97; H, 2.19; N, 4.40. Calcd: C, 47.38, H, 2.49, N, 4.61. IR (KBr pellet, cm^{−1}): 3421m(br), 1654s, 1601s, 1503m, 1428s, 1395vs, 1103m, 1018m, 865m, 845m, 750m, 730m, 637w.

X-ray Crystallographic Analysis. Diffraction data of the title complexes were collected on a Bruker SMART 1000 CCD area detector diffractometer with graphite-monochromatized Mo K α radiation ($\lambda = 0.71073$ Å) in ϕ and ω scan modes. All the structures were solved by direct methods using the program SHELXS 97 and refined by full-matrix least-squares methods on *F*² using the program SHELXL 97.⁸ All non-hydrogen atoms were refined anisotropically. Hydrogen atoms were placed in geometrically calculated positions. The crystallographic data and experimental details for structural analyses are summarized in Table 1. Selected bond lengths for complexes 1–6 are listed in Table 2.

Results and Discussion

Structure of 1. There is only one metal environment in 1 as shown in Figure 1. Eu(III) ion is eight-coordinated and surrounded by three oxygen atoms from three 1,2-BDC anions, two oxygen atoms from two HBDC anions, one oxygen atom from a coordinated water molecule, and two nitrogen atoms from one chelating phen molecule. The

distances of Eu–O range from 2.324 to 2.485 Å, and those of Eu–N are 2.628 and 2.654 Å. The average distance of Eu–O is 2.409 Å, which is strikingly shorter than that of Eu–N (2.641 Å). Two kinds of anions for H₂BDC, BDC, and HBDC exist in the asymmetric unit, and the coordination modes are shown in Chart 1 a,b.

The building block containing two europium ions is formed by symmetric operation on one asymmetric unit and thus is centrosymmetric. The distance between the two Eu ions is 4.159 Å. The two Eu ions in one building block are bridged by carboxylate groups from HBDC and BDC anions (see Chart 1a,b). The protonated carboxylate group of HBDC remains uncoordinated (see Chart 1a). Another carboxylate group of BDC is coordinated to one Eu ion from an adjacent building block with one oxygen atom, while the other oxygen atom of the carboxylate group remains free as shown in Chart 1b. So, the BDC anions connect building blocks to form a 2-D herringbone architecture with Z-shaped mosaics as shown in Figure 2.

Structure of 2. The asymmetric unit of 2 containing two kinds of metal environments is shown in Figure 3. Eu(1) ion is eight-coordinated by six oxygen atoms from five 1,3-BDC anions and two nitrogen atoms from chelating phen. Eu(2) ion is eight-coordinated as well, but surrounded by four oxygen atoms from four 1,3-BDC anions, two oxygen atoms from two coordinated water molecules, and two nitrogen atoms from a chelating phen. The average distance of Eu–N is 2.594 Å, while that of Eu–O is 2.405 Å. The dihedral angle between two phen groups is 44.9°. The separation of Eu(1) and Eu(2) is 8.525 Å.

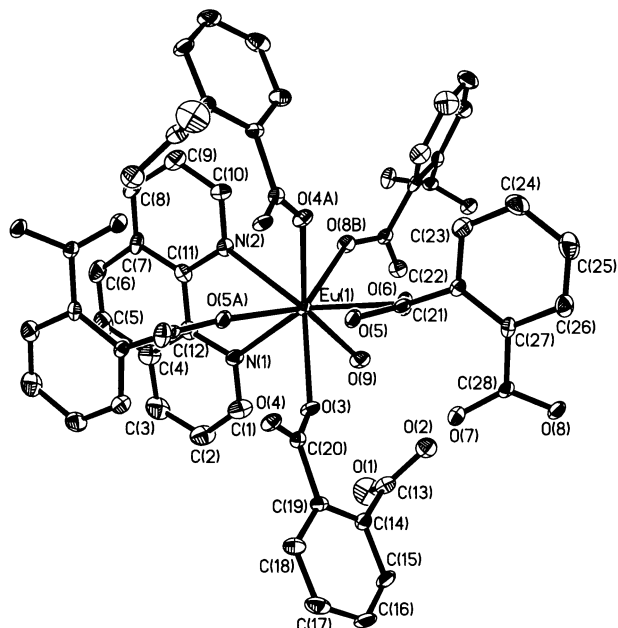
There are three crystallographically independent 1,3-BDC anions in 2. The dihedral angles between the benzene rings of three 1,3-BDC anions are 90.5°, 100.2°, and 157.9°. 1,3-BDC anions in 2 adopt two kinds of coordination modes as shown in Chart 1c,d. 1,3-BDC anions of the first type adopt a bridging and chelating mode (Chart 1c) to coordinate with Eu ions which are all crystallographically equivalent to Eu(2) in Figure 3, forming a set of rippled networks packed along

(8) Sheldrick, G. M. *SHELXS 97, Program for the Solution of Crystal Structure*; University of Göttingen: Göttingen, Germany, 1997. Sheldrick G. M. *SHELXL 97, Program for the Refinement of Crystal Structure*; University of Göttingen: Göttingen, Germany, 1997.

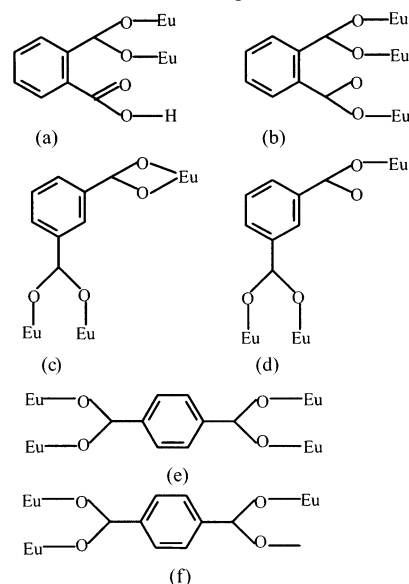
Table 2. Selected Bond Lengths (Å) for Complexes 1–6^a

| | | | | | | |
|---------------|-----------|--------------|-----------|---------------|-----------|--|
| | | | 1 | | | |
| Eu(1)–O(5)#1 | 2.324(4) | Eu(1)–O(4)#1 | 2.426(5) | Eu(1)–N(2) | 2.628(5) | |
| Eu(1)–O(8)#2 | 2.343(4) | Eu(1)–O(6) | 2.451(4) | Eu(1)–N(1) | 2.654(6) | |
| Eu(1)–O(3) | 2.425(4) | Eu(1)–O(9) | 2.485(5) | | | |
| | | | 2 | | | |
| Eu(1)–O(12)#1 | 2.355(3) | Eu(1)–N(2) | 2.572(4) | Eu(2)–O(9) | 2.429(3) | |
| Eu(1)–O(8)#2 | 2.377(3) | Eu(1)–N(1) | 2.624(4) | Eu(2)–O(14) | 2.454(3) | |
| Eu(1)–O(11) | 2.383(3) | Eu(2)–O(2)#4 | 2.339(3) | Eu(2)–O(13) | 2.459(3) | |
| Eu(1)–O(7)#3 | 2.394(3) | Eu(2)–O(1) | 2.359(3) | Eu(2)–N(3) | 2.574(4) | |
| Eu(1)–O(5) | 2.447(3) | Eu(2)–O(4)#5 | 2.359(3) | Eu(2)–N(4) | 2.606(4) | |
| Eu(1)–O(6) | 2.507(3) | | | | | |
| | | | 3 | | | |
| Eu(1)–O(6)#1 | 2.317(6) | Eu(1)–O(1) | 2.396(5) | Eu(1)–N(1) | 2.600(6) | |
| Eu(1)–O(3)#2 | 2.366(5) | Eu(1)–O(5) | 2.397(5) | Eu(1)–N(2) | 2.642(7) | |
| Eu(1)–O(2)#1 | 2.376(6) | Eu(1)–O(7) | 2.516(5) | | | |
| | | | 4 | | | |
| Yb(1)–O(12)#1 | 2.245(6) | Yb(1)–O(1) | 2.393(6) | Yb(2)–O(14) | 2.356(7) | |
| Yb(1)–O(5) | 2.258(7) | Yb(1)–O(7)#2 | 2.403(6) | Yb(2)–O(3)#2 | 2.423(7) | |
| Yb(1)–O(10) | 2.288(5) | Yb(2)–O(6) | 2.184(6) | Yb(2)–N(2) | 2.477(8) | |
| Yb(1)–O(11) | 2.310(6) | Yb(2)–O(9) | 2.296(6) | Yb(2)–N(1) | 2.474(7) | |
| Yb(1)–O(2) | 2.327(6) | Yb(2)–O(13) | 2.329(8) | | | |
| Yb(1)–O(8)#2 | 2.339(6) | Yb(2)–O(4)#2 | 2.340(6) | | | |
| | | | 5 | | | |
| Yb(1)–O(8)#1 | 2.205(8) | Yb(2)–O(1) | 2.269(9) | Yb(2)–N(1) | 2.571(10) | |
| Yb(1)–O(3) | 2.212(8) | Yb(2)–O(1)#7 | 2.269(9) | Yb(3)–O(6)#3 | 2.224(9) | |
| Yb(1)–O(4)#2 | 2.216(8) | Yb(2)–O(9) | 2.274(9) | Yb(3)–O(6) | 2.224(9) | |
| Yb(1)–O(7)#3 | 2.228(9) | Yb(2)–O(9)#7 | 2.274(9) | Yb(3)–O(10) | 2.231(9) | |
| Yb(1)–O(11)#4 | 2.269(10) | Yb(2)–O(5)#7 | 2.319(9) | Yb(3)–O(10)#3 | 2.231(9) | |
| Yb(1)–O(12)#5 | 2.293(9) | Yb(2)–O(5) | 2.319(9) | Yb(3)–O(2) | 2.292(9) | |
| Yb(1)–O(12)#4 | 2.671(9) | Yb(2)–N(1)#7 | 2.571(10) | Yb(3)–O(2)#3 | 2.292(9) | |
| | | | 6 | | | |
| Yb(1)–O(8)#1 | 2.155(5) | Yb(1)–N(2) | 2.511(6) | Yb(2)–O(1) | 2.296(5) | |
| Yb(1)–O(6) | 2.227(5) | Yb(1)–N(1) | 2.527(6) | Yb(2)–O(12) | 2.332(5) | |
| Yb(1)–O(11) | 2.265(5) | Yb(2)–O(3)#2 | 2.256(5) | Yb(2)–O(13) | 2.365(5) | |
| Yb(1)–O(9) | 2.266(5) | Yb(2)–O(10) | 2.279(5) | Yb(2)–N(3) | 2.502(6) | |
| Yb(1)–O(2) | 2.267(5) | Yb(2)–O(5) | 2.293(5) | Yb(2)–N(4) | 2.551(6) | |

^a Symmetry transformations used to generate equivalent atoms: **For 1**, #1, $-x + 1, -y, -z + 1$; #2, $x, -y + 1/2, z - 1/2$; #3, $x, -y + 1/2, z + 1/2$. **For 2**, #1, $-x, -y + 1, -z + 1$; #2, $x, -y + 1/2, z + 1/2$; #3, $-x, y + 1/2, -z + 1/2$; #4, $-x + 1, -y + 2, -z + 1$; #5, $x, y - 1, z$. **For 3**, #1, $-x + 1, -y + 2, -z + 2$; #2, $x + 1, y + 1, z$. **For 4**, #1, $-x + 2, -y + 1, -z + 1$; #2, $-x + 1, -y + 1, -z + 1$. **For 5**, #1, $-x + 1/2, -y + 1/2, z + 1/2$; #2, $x - 1/2, -y + 1/2, -z + 1$; #3, $-x, y, -z + 1/2$; #4, $-x + 1/2, y + 1/2, -z + 1/2$; #5, $-x, -y, z + 1/2$; #6, $x + 1/2, -y + 1/2, -z + 1$; #7, $-x + 1, y, -z + 1/2$. **For 6**, #1, $-x, -y + 1, -z + 1$; #2, $-x + 1, -y + 1, -z$.

**Figure 1.** Asymmetric unit of **1** with 40% thermal ellipsoids. All the hydrogen atoms are omitted for clarity.

the *a* axis (see Figure 4a). In the 2-D network, there are two types of rings. One is an eight-membered ring composed of two carboxylate groups and two Eu(III) ions. The other is a

Chart 1. Coordination Modes in Complexes 1–3

32-membered ring formed by four 1,3-BDC groups bridging four Eu(III) ions (see Figure 4a).

1,3-BDC anions of the other type are coordinated to Eu(III) ions through three oxygen atoms of the carboxylate groups (Chart 1d) and form 2-D networks parallel to the *ab* plane

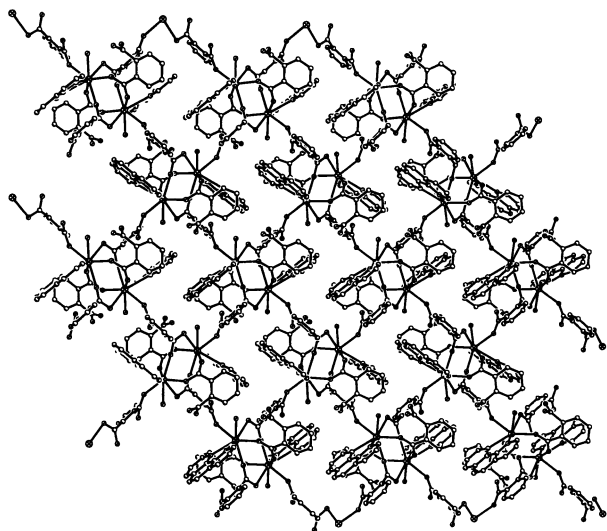


Figure 2. Packing diagram of **1** viewed along the *a* axis. All the hydrogen atoms are omitted for clarity.

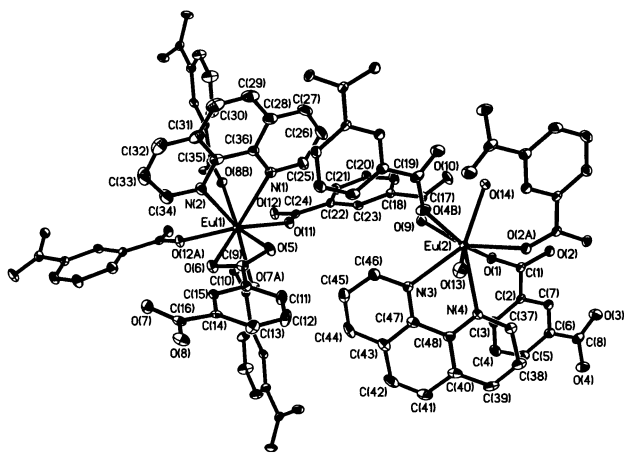


Figure 3. Asymmetric unit of **2** with 40% thermal ellipsoids. Lattice water molecules and all the hydrogen atoms are omitted for clarity.

(Figure 4b). From Figure 4b, it can be seen that there are three kinds of grids: 8-membered, 16-membered, and 48-membered rings. 2-D networks of the two types shown in Figure 4 intersect at Eu(III) ions crystallographically equivalent to Eu(2) and thus form a 3-D network.

Structure of 3. The coordination environment of the Eu ion in **3** is shown in Figure 5. The Eu(III) ion is eight-coordinated. Five oxygen atoms belonging to five 1,4-BDC anions and another one from a coordinated water molecule are coordinated to the Eu(III) ion. The last two coordination sites are occupied by two nitrogen atoms from a chelating phen. As expected, the average distance of Eu–O (2.395 Å) is much shorter than that of Eu–N (2.621 Å).

In **3**, 1,4-BDC anions adopt two kinds of coordination modes as shown in Chart 1: bridging and bridging (e), and monodentate and bridging (f). As shown in Figure 6, each dimeric block composed of two Eu(III) ions with a separation of 4.333 Å is bridged by six 1,4-BDC groups with four adjacent dimeric blocks, which results in a 2-D infinite network. The 2-D structure comprises infinite rhombus grids with a cavity of ca. 10.3×10.8 Å. Each grid contains eight Eu(III) ions, four of those lying in a plane, the others

distributed in another one. We found that all the Eu(III) ions in **3** are distributed in two perfect planes with a mean deviation from the plane of 0.0 Å. And the two Eu(III) ion planes are parallel to each other. The dihedral angle between the phen plane and Eu(III) ion plane is 110.9°.

A 3-D supramolecular network results from the hydrogen bonds formed between the uncoordinated oxygen atoms belonging to carboxylate groups and uncoordinated water molecules from adjacent layers: $D_{[O(7)\cdots O(4)]} = 2.854$ Å (symmetry code *i*: $-x, -y + 1, -z + 1$), $d_{[O(4)]\cdots H(1)} = 2.070$ Å, and $\theta_{[O(7)-H(1)\cdots O(4)]} = 141.3^\circ$.

Structure of 4. Two types of coordinated environments of Yb(III) ions in **4** are found as shown in Figure 7. Yb(1) is eight-coordinated and surrounded by eight oxygen atoms from five 1,2-BDC anions. Yb(2) is eight-coordinated and has a N_2O_6 environment by virtue of four oxygen atoms from three 1,2-BDC anions, two oxygen atoms from two coordinated water molecules, and two nitrogen atoms of one chelating phen. The average distance of Yb–N is 2.476 Å, which is much larger than that of Yb–O (2.321 Å). The distance between Yb(1) and Yb(2) is 4.609 Å.

Three crystallographically independent 1,2-BDC anions existing in **4** adopt three types of coordination modes (Chart 2a–c) and play different roles in the formation of the coordination polymer (see Figure 8). The 1,2-BDC anion of the first type adopts mode a (Chart 2) to coordinate with two Yb ions belonging to two asymmetric units in the chelating mode, and the 1,2-BDC anion of the second type adopts mode b (Chart 2) to coordinate to three Yb ions from the two asymmetric units. Then the two types of 1,2-BDC anions which adopt modes a and b connect Yb ions to form a four-metal building block, and the four-metal blocks are connected into a 1-D polymeric chain (see Figure 8) via the 1,2-BDC of the third type adopting mode c (Chart 2). In this chain, the Yb(III) ions are coplanar and have a mean deviation of ca. 0.0067 Å from the plane. The dihedral angles between the Yb ion plane and the aromatic ring of three types of 1,2-BDC anions are 20.8°, 90.4°, and 96.2°. It is worth noting that the Yb(III) ions of one chain distribute in a strip with a width of ca. 6.9 Å. The phen molecules arrange on both sides of the strip and extend the strip to a broader region (17.5 Å). A 3-D network is constructed by several kinds of hydrogen bonds: (a) hydrogen bonding among lattice water molecules (O \cdots O distance 2.649–2.878 Å); (b) hydrogen bonding between lattice water molecules and carboxylate oxygen atoms (O \cdots O distance 2.614–2.784 Å); (c) hydrogen bonding between lattice water molecules and C–H of phen molecules (C \cdots O distance 3.072 and 3.358 Å); (d) hydrogen bonding of C–H of phen molecules and the carboxylate oxygen atoms (C \cdots O distance 3.156 Å).

Structure of 5. There are three kinds of metal environments in **5** as shown in Figure 9. Yb(1) is seven-coordinated by seven oxygen atoms from six 1,3-BDC anions. Yb(2) is eight-coordinated by six oxygen atoms from six 1,3-BDC anions and two nitrogen atoms from one chelating phen molecule, and Yb(3) is six-coordinated by six oxygen atoms from six 1,3-BDC anions. The distances of Yb \cdots Yb are Yb(1) \cdots Yb(2) = 10.203 Å, Yb(1) \cdots Yb(3) = 8.361 Å, and

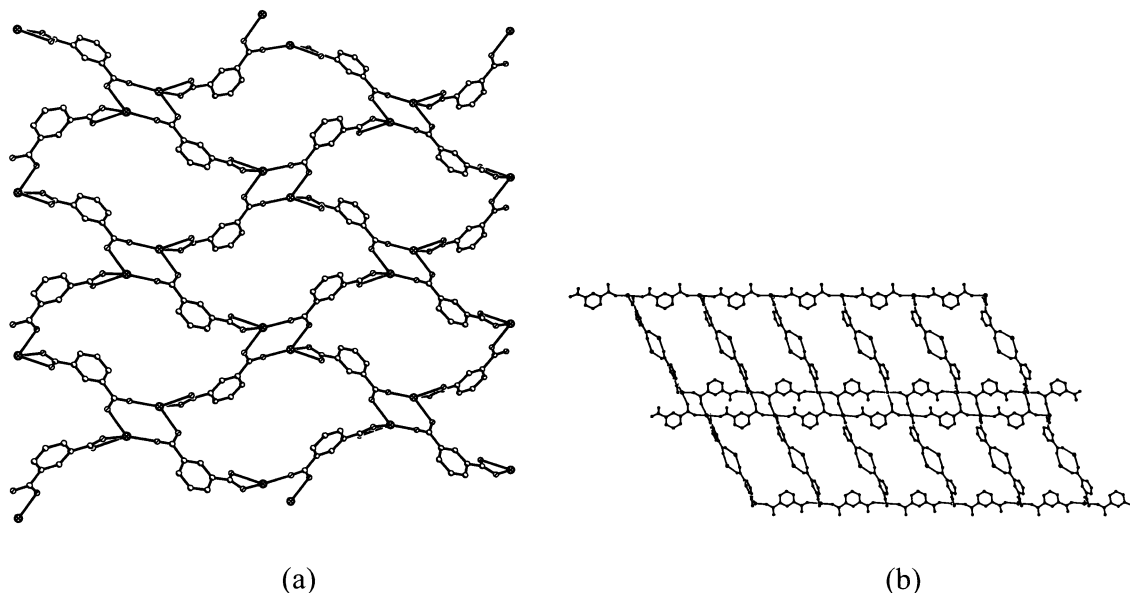


Figure 4. (a) 2-D network (viewed along the *a* axis) formed by 1,3-BDC anions linking Eu ions via adopting coordination mode *c* in Chart 1. Other 1,3-BDC anions and hydrogen atoms are omitted for clarity. (b) 2-D network (viewed along the *c* axis) formed by 1,3-BDC anions linking Eu ions via adopting coordination mode *d* in Chart 1. Other 1,3-BDC anions and hydrogen atoms are omitted for clarity.

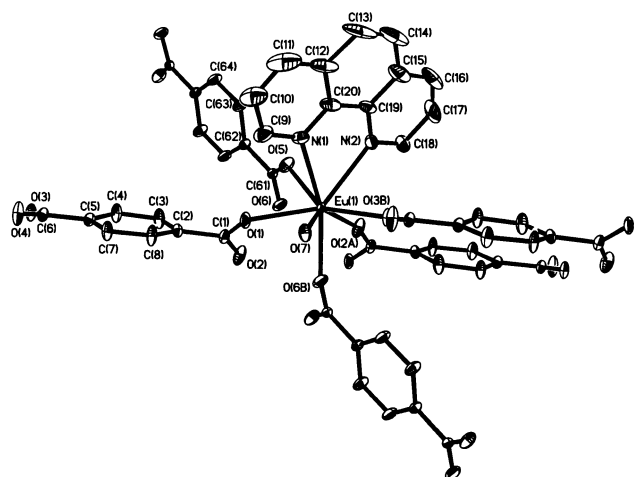


Figure 5. Asymmetric unit of **3** with 40% thermal ellipsoids. All the hydrogen atoms are omitted for clarity.

$\text{Yb}(2)\cdots\text{Yb}(3) = 4.399 \text{ \AA}$. It is worth noting here that Yb(2) and Yb(3) ions stand exactly on the 2-fold axis parallel to the *b* axis and arrange alternately along the 2-fold axis with separations of $\text{Yb}\cdots\text{Yb} = 13.875$ and 10.622 \AA , respectively.

1,3-BDC anions in **5** adopt two kinds of coordination modes (Chart 2d,e). Figure 10 shows the undulating layers which are bridged by 1,3-BDC anions connecting Yb ions in tetradentate (Chart 2d) and pentadentate (Chart 2e) coordination modes. As shown in Figure 10a, 1,3-BDC anions adopting the tetradentate mode act as bridges to connect Yb(III) ions, thus forming a wavelike double layer in which two layers twist together. The other 1,3-BDC anions adopt the pentadentate coordination mode to coordinate with Yb ions and form a series of wavelike layers, which seem like sine curves viewed along the *a* axis (Figure 10b). The 3-D network structure of **5** can be considered to be assembled by the two kinds of 2-D layers (shown in Figure 10) via the coordination bonds between carboxylate oxygen atoms and Tb ions. The packing diagram of **5** is shown in Figure 11.

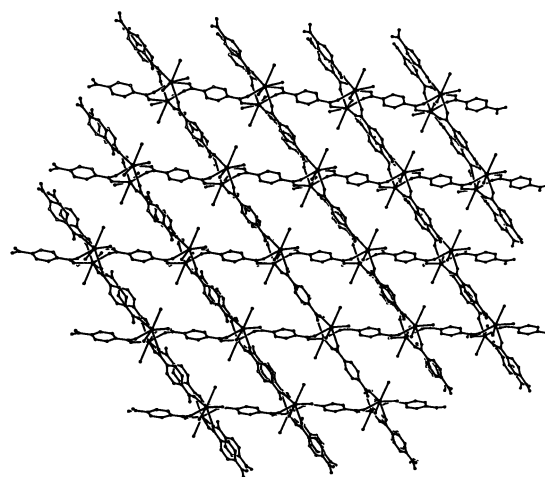


Figure 6. Packing diagram of **3** viewed along the *c* axis. Carbon atoms of phen molecules and all the hydrogen atoms are omitted for clarity.

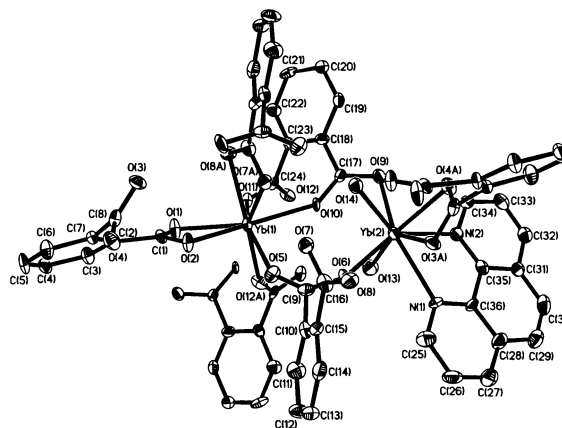
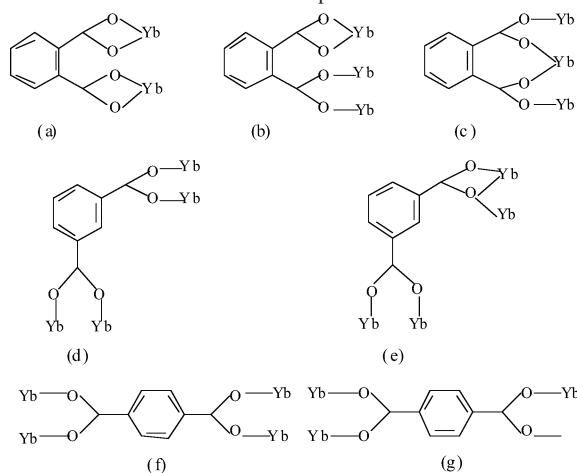


Figure 7. Asymmetric unit of structure of **4** with 40% thermal ellipsoids. Lattice water molecules and all the hydrogen atoms are omitted for clarity.

Structure of 6. Two crystallographically independent ytterbium ions exist in **6**. As shown in Figure 12, Yb(1) is seven-coordinated by five oxygen atoms from five 1,4-BDC

Chart 2. Coordination Modes in Complexes 4–6



anions and two nitrogen atoms from a chelating phen molecule; Yb(2) is eight-coordinated by five oxygen atoms from five 1,4-BDC anions, one oxygen atom from one coordinated water molecule, and two nitrogen atoms belonging to phen. The distance of Yb(1)⋯Yb(2) is 4.189 Å.

Each asymmetric unit of $[\text{Yb}_2(1,4\text{-BDC})_3(\text{phen})_2(\text{H}_2\text{O})]$ connects four neighboring asymmetric units via 1,4-BDC ligands, and thus, a 2-D infinite network is formed (see Figure 13). The 2-D network is parallel to the *ac* plane and has rhombus grids with a cavity of ca. 11×11 Å. Similar to **3**, all the Yb(III) ions in a 2-D network are not coplanar but are distributed in two parallel planes which both have an average atomic displacement of 0.0607 Å. The distance between the two planes is ca. 3.5 Å. Phen molecules lie up and down the layer, and the dihedral angles between the plane of Yb(III) ions and the phen plane are ca. 113.0° and 113.9° , respectively.

There are two types of 1,4-BDC anions in **6**. (1) Each 1,4-BDC anion acts as a bridge and coordinates to Yb(III) ions with all four oxygen atoms (Chart 2f). (2) The 1,4-BDC anion bonds to Yb(III) ions with three oxygen atoms, and one oxygen atom remains uncoordinated (Chart 2g). Part of the uncoordinated oxygen atoms form C–H⋯O hydrogen bonds with C–H of phen molecules ($\text{C}\cdots\text{O} = 3.004$ Å) and O–H⋯O hydrogen bonds with coordinated water molecules ($\text{O}\cdots\text{O} = 2.764$ Å) in the crystal, resulting in a 3-D supramolecular structure.⁹ In addition, weak π – π aromatic interactions exist between the phen molecules of neighboring layers, the average distance between two phen planes is 3.5 Å, and the dihedral angle is 2.2° .¹⁰

The above results show that BDC anions are good links for constructing high-dimensional networks for lanthanides. The six complexes possess a 2-D network (**1**) or 3-D networks (**2**–**6**). Two kinds of 3-D networks are sustained by coordination bonds (**2** and **5**), while other 3-D networks are formed via hydrogen bonds and/or π – π interactions connecting 1-D chains for **4** or 2-D layers for **3** and **6**. Owing

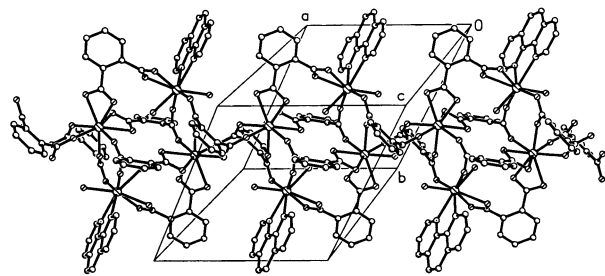


Figure 8. Packing diagram of **4**. All the hydrogen atoms are omitted for clarity.

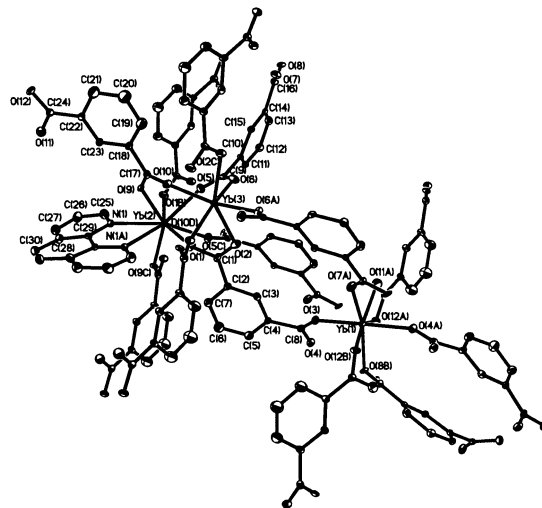


Figure 9. Asymmetric unit of **5** with 40% thermal ellipsoids. All the hydrogen atoms are omitted for clarity.

to their larger radii, Eu(III) and Yb(III) ions have higher coordination numbers than transition-metal ions, and thus, the BDC anions tend to adopt varied coordination modes to coordinate with Eu(III) and Yb(III) ions to saturate their coordination sites. The results also indicate that different substitution positions of the two carboxyl groups on the benzene ring take an important role in the formation of different structures. Rodlike rigid 1,4-BDC is a good spacer and is widely used in the construction of a 3-D network with channels^{2,11} because of its linear and divergent attribution. When 1,4-BDC is not the only ligand in the formation of complexes, the crystal structures are determined by not only 1,4-BDC but also other ligands and metal centers. For example, when 1,4-BDC as well as 4,4'-bipy is involved in the formation of a coordination polymer,¹² 1,4-BDC ligands bridge metal centers to form 2-D rectangular or parallelogram-like sheets; then adjacent sheets are further linked by 4,4'-bipy and thus form 3-D networks. When 1,10-phen is used instead of 4,4'-bipy,¹³ the crystal structures are different as the metal centers are varied. 1,10-Phen chelates to metals, while 1,4-BDC ligands link metal centers to form 1-D zigzag chains (Co, Cu, Zn) or 3-D networks (Mn, Cd) with channels. In the title complexes, 1,4-BDC ligands link

(9) (a) Desiraju, G. R. *Acc. Chem. Res.* **1996**, *29*, 441–449. (b) Biradha, K.; Nangia, A.; Desiraju, G. R.; Carrell, C. J.; Carrell, H. L. *J. Mater. Chem.* **1997**, *7*, 1111–1122.

(10) Janiak, C. *J. Chem. Soc., Dalton Trans.* **2000**, 3885–3896.

(11) Dai, J.-C.; Wu, X.-T.; Fu, Z.-Y.; Hu, S.-M.; Du, W.-X.; Cui, C.-P.; Wu, L.-M.; Zhang, H.-H.; Sun, R.-Q. *Chem. Commun.* **2002**, 12–13.

(12) Tao, J.; Tong, M.-L.; Chen, X.-M. *J. Chem. Soc., Dalton Trans.* **2000**, 3669–3674.

(13) Sun, D.-F.; Cao, R.; Liang, Y.-C.; Shi, Q.; Su, W.-P.; Hong, M.-C. *J. Chem. Soc., Dalton Trans.* **2001**, 2335–2340.

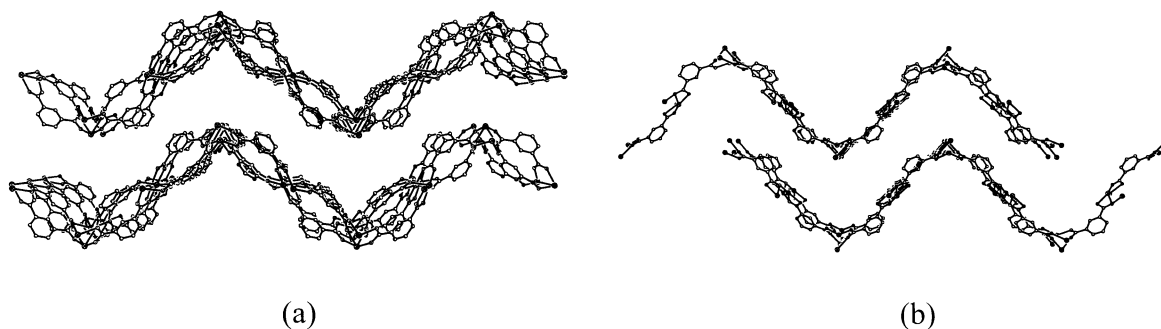


Figure 10. 2-D undulating layers viewed along the *a* axis: (a) formed by 1,3-BDC anions bridging Yb ions in the tetradentate coordination mode (Chart 2d); (b) formed by 1,3-BDC anions linking Yb ions in the pentadentate coordination mode (Chart 2e).

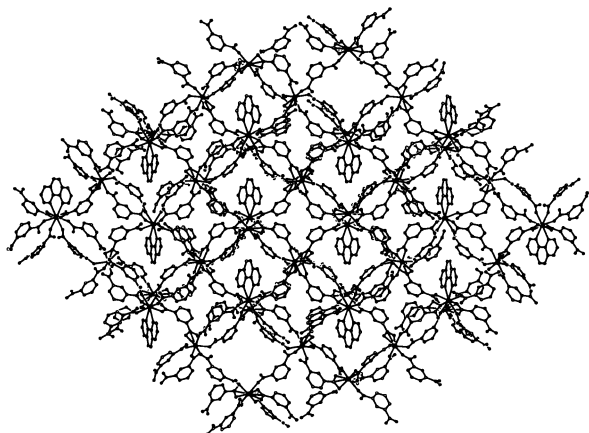


Figure 11. Packing diagram of **5** viewed along the *a* axis. All the hydrogen atoms are omitted for clarity.

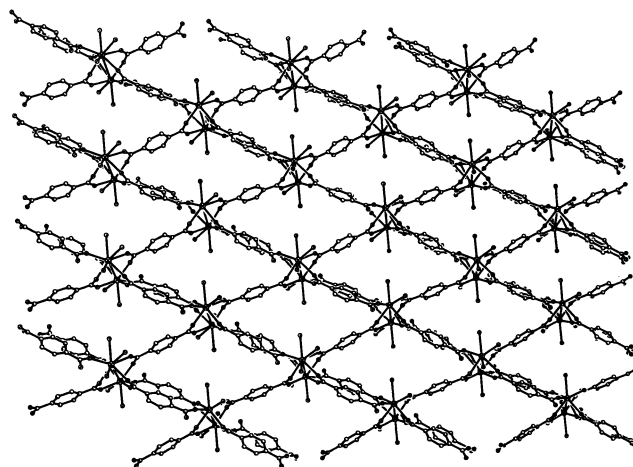


Figure 13. Packing diagram of **6** viewed along the *b* axis. Carbon atoms of phen molecules and all the hydrogen atoms are omitted for clarity.

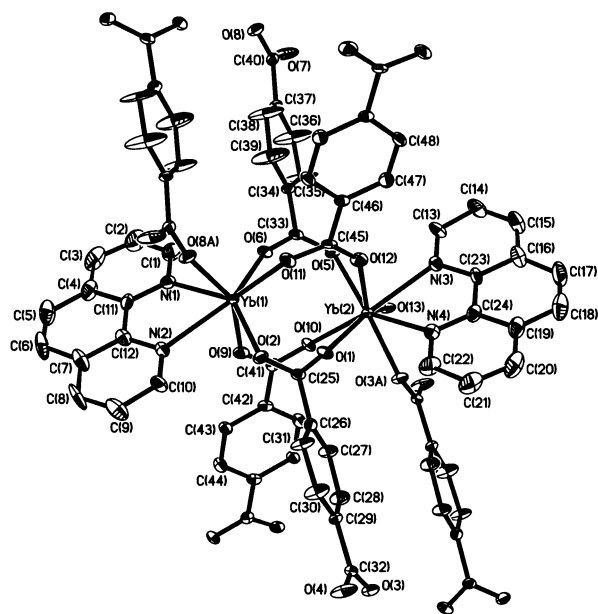


Figure 12. Asymmetric unit of **6** with 40% thermal ellipsoids. All the hydrogen atoms are omitted for clarity.

Eu or Yb to form 2-D layers with rhombus grids. 1,3-BDC with 120° between two carboxylate groups is apt to link metal centers at 120° . As reported by Zaworotko,^{3b} for the transition-metal coordination polymers, 1,3-BDC links square SBUs (second building units) at 120° and forms a 2-D infinite framework. However, in this study, 1,3-BDC ligands connect Eu and Yb ions and form 3-D networks. The angle between

two carboxylate groups of 1,2-BDC is the smallest among those of three isomers, and the distance between two carboxylate groups is the closest. So, as expected 1,2-BDC is not as good as 1,4-BDC and 1,3-BDC for constructing 3-D networks. To the best of our knowledge, 3-D crystal structures containing 1,2-BDC as a link are rarely reported,¹⁴ while 1-D chains and 2-D layer structures containing it are commonly encountered in the references. Nevertheless, **1** and **4** have 2-D and 3-D networks, respectively.

One phen molecule occupies two coordination sites by adopting the chelating mode, which may lead to lower dimensionality of coordination polymers. However, phen can also construct supramolecular architecture with higher dimensional structures by forming C–H \cdots O hydrogen bonds and π – π aromatic interactions. This can be inferred from the comparison of the title complexes with the reported binary lanthanide benzenedicarboxylate complexes. The binary ytterbium 1,2-benzenedicarboxylate complex shows a 2-D network;^{7d} when phen is introduced into the structure (**4**), it displays 1-D nanochains which are further connected to form a 3-D network via hydrogen bonds. All binary lanthanide (Eu, Tb, Er) 1,4-benzenedicarboxylate complexes reported⁵ are 3-D networks sustained by coordination bonds. Similarly, both **3** and **6** are composed of layers, and then 3-D supramolecular structures are formed by hydrogen bonds

(14) Lightfoot, P.; Snedden, A. *J. Chem. Soc., Dalton Trans.* **1999**, 3549–3551.

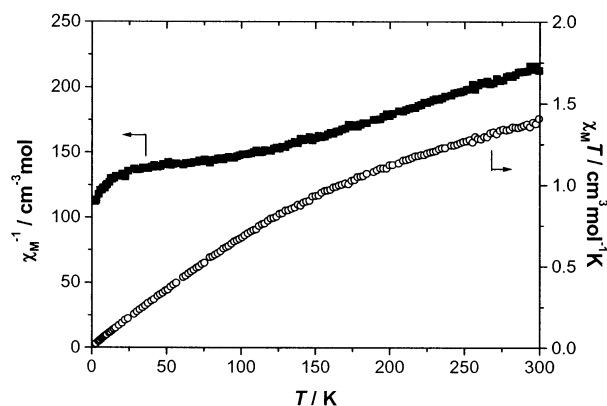


Figure 14. Temperature dependence of $\chi_M T$ (○) and χ_M^{-1} (■) of **1**.

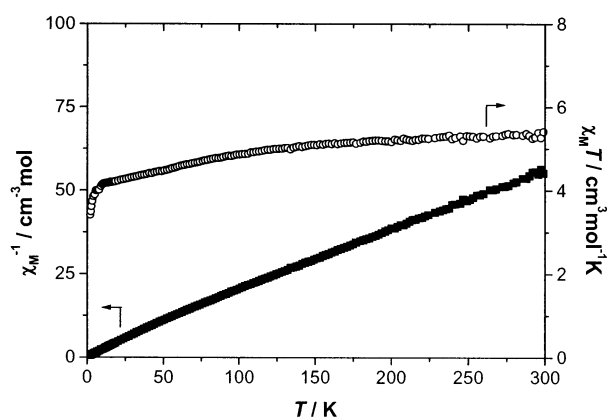


Figure 15. Temperature dependence of $\chi_M T$ (○) and χ_M^{-1} (■) of **4**.

and/or π – π aromatic interactions. The effect of phen on the construction of supramolecular structures may be of high interest for the design of advanced supramolecular materials.

Magnetic Properties. The temperature dependence of the magnetic susceptibility of **1** is shown in Figure 14, where χ_M is the corrected molar magnetic susceptibility per Eu(III) ion. The observed $\chi_M T$ at room temperature is $1.41 \text{ cm}^3 \text{ mol}^{-1} \text{ K}$, slightly less than the value 1.5 for a Eu(III) ion calculated by Van Vleck allowing for population of the excited state with higher values of J at 293 K. As the temperature is lowered, $\chi_M T$ decreases continuously, which should be attributed to the depopulation of the Stark levels for a single Eu(III) ion. At the lowest temperature, $\chi_M T$ is close to zero, indicating a $J = 0$ ground state of the Eu(III) ion (7F_0). The magnetic susceptibility above 150 K follows the Curie–Weiss law due to the presence of thermally populated excited states.

The temperature dependence of the magnetic susceptibility of **4** is displayed in Figure 15, where χ_M is the corrected molar magnetic susceptibility per $[\text{Yb}_2]$ unit. At room temperature, the value of $\chi_M T$ is $5.21 \text{ cm}^3 \text{ mol}^{-1} \text{ K}$, which is close to the calculated value for two Yb free ions ($5.15 \text{ cm}^3 \text{ mol}^{-1} \text{ K}$). Upon cooling, $\chi_M T$ decreases steadily, and fast at low temperature. This results primarily from the splitting of the ligand field of the Yb(III) ion together with the possible contribution of the weak antiferromagnetic coupling between Yb(III) ions, considering a possible interaction path through two carboxylate bridges with a 4.609 \AA Yb–Yb distance. The magnetic susceptibility above 100

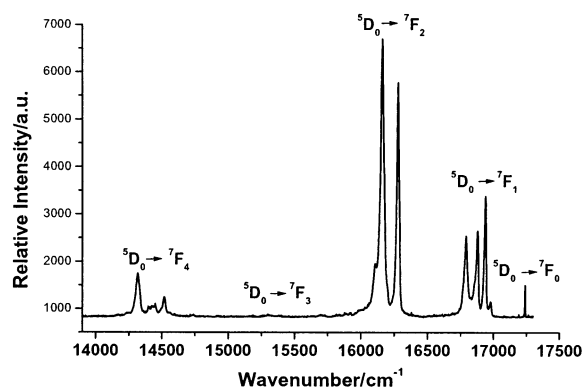


Figure 16. Luminescence spectrum of **1** at 77 K, $\lambda_{\text{exc}} = 355 \text{ nm}$.

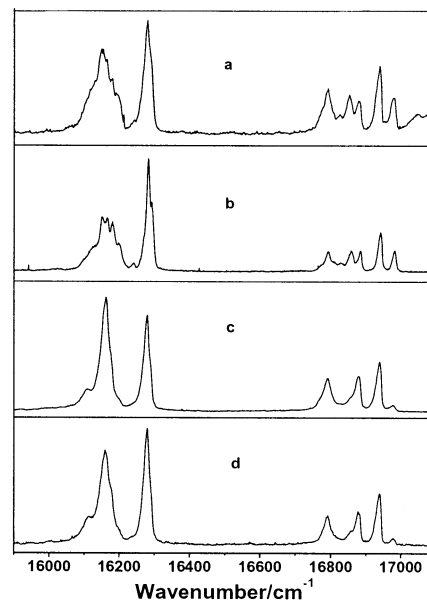


Figure 17. Time-resolved spectra of **1** at 77 K, $\lambda_{\text{exc}} = 355 \text{ nm}$. Delay time: (a) 5 μs , (b) 25 μs , (c) 50 μs , (d) 500 μs .

K obeys the Curie–Weiss law with the Weiss constant $\Theta = -15 \text{ K}$ and the Curie constant, $C = 5.59 \text{ cm}^3 \text{ mol}^{-1} \text{ K}$. The C value corresponds to an effective magnetic moment of $4.73 \mu_B$ per Yb(III) ion. The field dependence of the magnetization of **4** is investigated at 1.78 K in the range of 0–50 kOe. The magnetization increases slowly as the field increases and nearly reaches saturation ($4.65 N\beta$) at 50 kOe.

Photophysical Properties. Complex **1** exhibits intense red fluorescence under UV light. The luminescence spectrum of **1** corresponding to $^5D_0 \rightarrow ^7F_J$ ($J = 0-4$) transitions in the range of $13900-17300 \text{ cm}^{-1}$ is shown in Figure 16. One narrow peak at 17240 cm^{-1} is assigned to the $^5D_0 \rightarrow ^7F_0$ transition. It is well-known that the $^5D_0 \rightarrow ^7F_2$ transition induced by the electric dipole moment is hypersensitive to the environment of the Eu(III) ion, while the $^5D_0 \rightarrow ^7F_1$ transition is a magnetic dipole transition which is fairly insensitive to the coordination environment of the Eu(III) ion. The intensity ratio $I(^5D_0 \rightarrow ^7F_2)/I(^5D_0 \rightarrow ^7F_1)$ is equal to 2.22, which indicates that the symmetry of the Eu(III) ion site is low.¹⁵ This is in agreement with the result of the single-crystal X-ray analysis.

Figure 17 shows the time-resolved spectra recorded in the range of $15900-17100 \text{ cm}^{-1}$. We found that spectra a and

b are similar, while spectrum c is similar to spectrum d. However, in comparison of spectrum a (or b) with spectrum c (or d) in the range of 16700–17100 cm^{-1} ($^5\text{D}_0 \rightarrow ^7\text{F}_1$ transition), components of spectrum a (or b) are more than those of spectrum c (or d), which can be attributed to the emission from the $^5\text{D}_1$ excited state ($^5\text{D}_1 \rightarrow ^7\text{F}_3$ transition). The $^5\text{D}_1$ level has a much shorter lifetime than the $^5\text{D}_0$ level. Therefore, when the delay time is prolonged, some bands originating from the $^5\text{D}_1$ level disappear. The emission spectra of the $^5\text{D}_0 \rightarrow ^7\text{F}_2$ transition shown in Figure 17 are not well resolved, which can be attributed to the slightly

different environment of the Eu(III) ion in **1** and thus resulting in the overlap of the components of the $^5\text{D}_0 \rightarrow ^7\text{F}_2$ emission. This is commonly observed in europium coordination polymers.

Acknowledgment. This work is supported by the National Natural Science Foundation of China (Grants 29971005 and 20071004) and the Key State Project of Fundamental Research (Grant G 1998061308).

Supporting Information Available: Crystallographic data for six complexes in CIF format. This material is available free of the charge via the Internet at <http://pubs.acs.org>.

(15) Bünzli, J.-C. G. In *Lanthanide Probes in Life, Chemical and Earth Sciences. Theory and Practice*; Bünzli, J.-C. G., Choppin, G. R., Eds.; Elsevier Scientific Publishers: Amsterdam, 1989; Chapter 7.

IC034258C